CHAPTER 7
TLCD EXPERIMENTS

In theory, there is no difference between theory and practice.
But, in practice, there is.
- Jan L.A. Van de Snepscheut

In this chapter, different experiments conducted using scale models of structures along with a prototype semi-active TLCD are presented. First, the dynamic characteristics of the combined structure-damper system were compared with previously obtained analytical results reported in Chapter 3. Next, a gain-scheduled control law based on a prescribed look-up table was experimentally verified for achieving the optimum damping based on a prescribed look-up table.

7.1 Introduction

Experimental studies using tuned liquid column dampers (TLCDs) for evaluating their control performance have been limited to passive systems. Sakai *et al.* (1991) verified the performance of a TLCD installed on a scaled-down model of an actual cable stayed bridge tower. Balendra *et al.* (1995) conducted shaking table tests using TLCDs and studied the effect of different orifice opening ratios on the liquid motion. Experimental studies have also been reported by Hitchcock *et al.* (1997) using passive TLCDs with no orifice, termed as liquid column vibration absorbers (LCVAs). Recently Xue *et al.* (2000) presented experimental studies on the application of a passive TLCD in suppressing the pitching motion of structures and conducted experiments to delineate the influence of different damper parameters on the TLCD performance.

A full scale installation of a bi-directional passive liquid column vibration absorber (LCVA) on a 67m steel frame communications tower has been reported by Hitchcock *et al.* (1999). This device does not have an orifice/valve in the U-tube and hence, it is not possible to control the damping in the LCVA. The authors also acknowledge that due to the lack of orifice, the damping ratio of the LCVA was not expected to be optimum. The authors observed that the LCVA did not perform optimally at all wind speeds. Response reduction of almost 50% was noted, however, non-optimal performance of the damper was noted above and below the design wind speed. This observation re-affirms the fact that passive liquid damper systems are inadequate in performing optimally at all levels of excitation (Kareem, 1994).

This chapter discusses experimental verification of a semi-active system which may be utilized to overcome the aforementioned shortcomings of a passive TLCD system. Although researchers have studied the semi-active version of TLCD theoretically (Haroun et al. 1994; Kareem, 1994; Abe *et al.* 1996; Yalla *et al.* 1998), there has been no reported experimental verification of such a system. In this chapter, different experiments were conducted using scale models of structures along with a prototype semi-active TLCD. The dynamic characteristics of the coupled structure-damper system were compared to previously obtained analytical results presented in Chapter 3. Next, a gain-scheduled control law for achieving the optimum damping based on a prescribed look-up table was verified experimentally.

7.2 Experimental Studies

The experimental set-up is shown in Fig. 7.1(a)-(b). It consists of a single story structure model attached to a TLCD. The TLCD consists of a U-shaped tube made of PVC

material with an electro-pneumatic actuator driving a ball valve attached at the center of the tube.

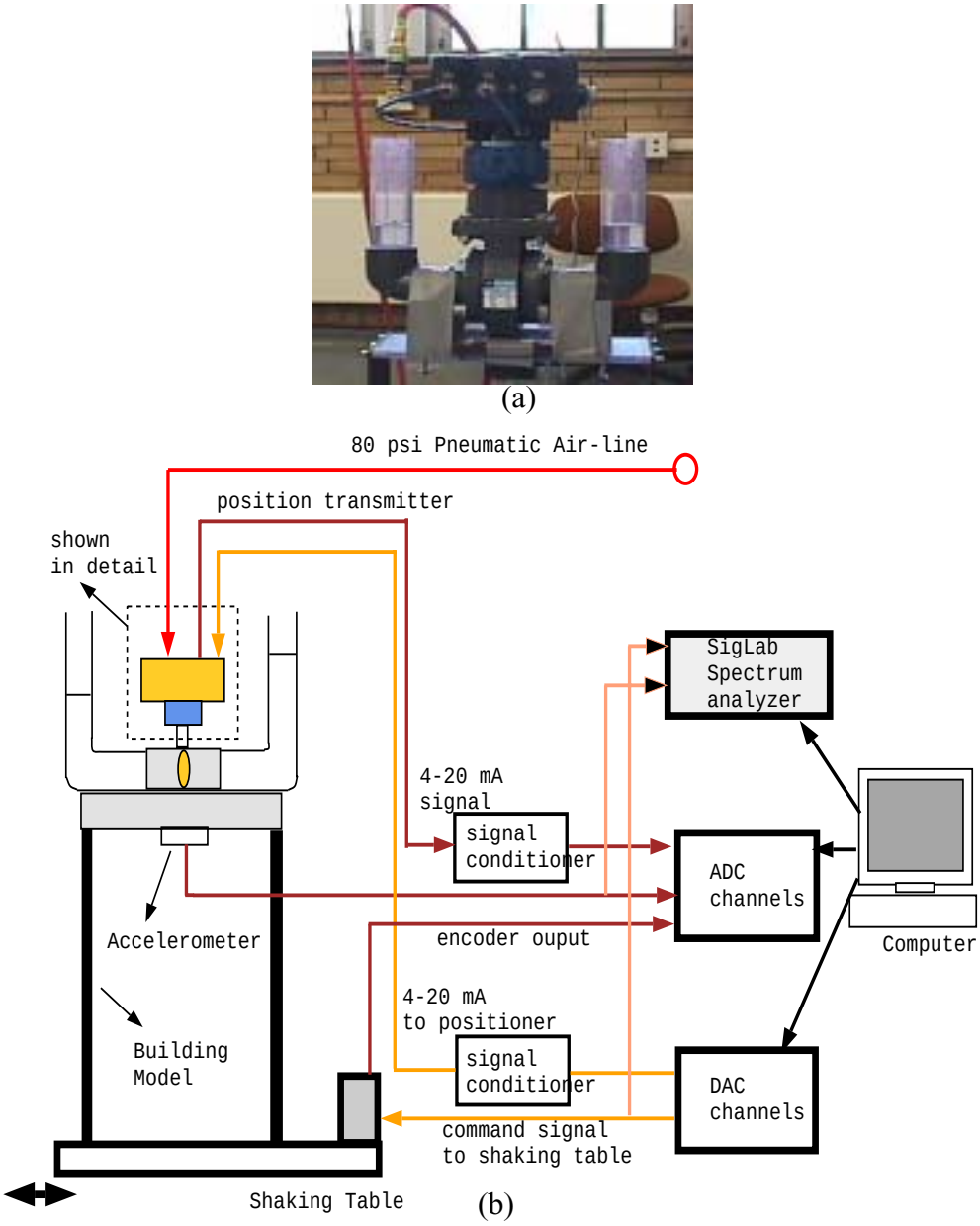

Figure 7.1 (a) Photograph of the Electro-pneumatic actuator (b) Schematic diagram of the experimental set-up

The U-tube has a circular cross-section with an inner diameter of 3.8 cm and a horizontal length of 35.5 cm and a total length of 81 cm. The valve used in this study is a

ball valve of 3.8 cm (1.5 inches) diameter. A command voltage changes the valve opening angle (θ), which effectively changes the orifice area of the valve. The details of the valve characteristics are presented in Appendix A.3, where the valve opening angle is related to the headloss coefficient(ξ).

Transfer function measurements were obtained by exciting the shaking table with a band-limited random white noise (cutoff frequency f_c = 2 Hz), at different levels of excitation amplitudes and the acceleration was measured at the top of the structure. The excitation amplitude in these experimental studies is referred to as S_0 and it represents an RMS value of excitation (in volts). The range of feasible RMS excitation displacement amplitudes of the shaking table without spilling water out of the U-tube was varied between 0.05-0.3 volts.

The model structure without the damper is a linear system, which was confirmed through identification of the transfer function at different amplitudes of excitation. The effect of the pneumatic actuator used to drive the valve in the TLCD on the dynamics of the structure was found to be negligible. This was done by comparing the transfer functions with and without the air-supply to the pneumatic actuator. All transfer function measurements were obtained using SigLab^{TM} spectrum analyzer using the average of 15 measurements. From the transfer function and free vibration decay curves, the natural frequency and damping ratio of the uncontrolled building was determined to be 0.92 Hz and 0.6%, respectively. The mass ratio (ratio of the liquid mass in the damper to the first modal mass of the structure) is kept approximately 10% of the total mass of the structure.

7.2.1 Effect of tuning ratio

The tuning ratio (γ) is defined as the ratio of the natural frequency of the damper ($=\sqrt{2g/l}$) to the natural frequency of the structure. In order to determine the optimum tuning ratio, liquid columns of different lengths were considered. Figure 7.2 (a) shows the transfer function with different tuning ratios. The $\|H\|_2$ norm was used as a measure of evaluating the performance at each tuning ratio, which is defined as:

$$\|H\|_2 \approx \int_{\omega_a}^{\omega_b} \left| H_{\ddot{X}_s \ddot{x}_g}(\omega) \right|^2 d\omega \tag{7.1}$$

where $\ddot{X}_s$ is the acceleration of the structure, $\ddot{x}_g$ is the ground acceleration of the shaking table, ω_a=0.5 Hz and ω_b=1.5 Hz. The range of frequencies were limited to 0.5-1.5 Hz because below 0.5 Hz there was a lot of noise in the system and above 1.5 Hz, there is negligible change in each transfer function.

Figure 7.2 (b) shows the variation of the H_2 norm as a function of the tuning ratio. A fourth order polynomial fit was used to determine the optimum tuning ratio as equal to 0.953. This corresponds to a liquid length of 25 inches (63.5 cm). One can observe that the two peaks in the transfer function are almost equal in height at the optimum tuning. This is consistent with the analytical formulations regarding optimal tuning of two-degree-of-freedom systems (Den Hartog, 1940).

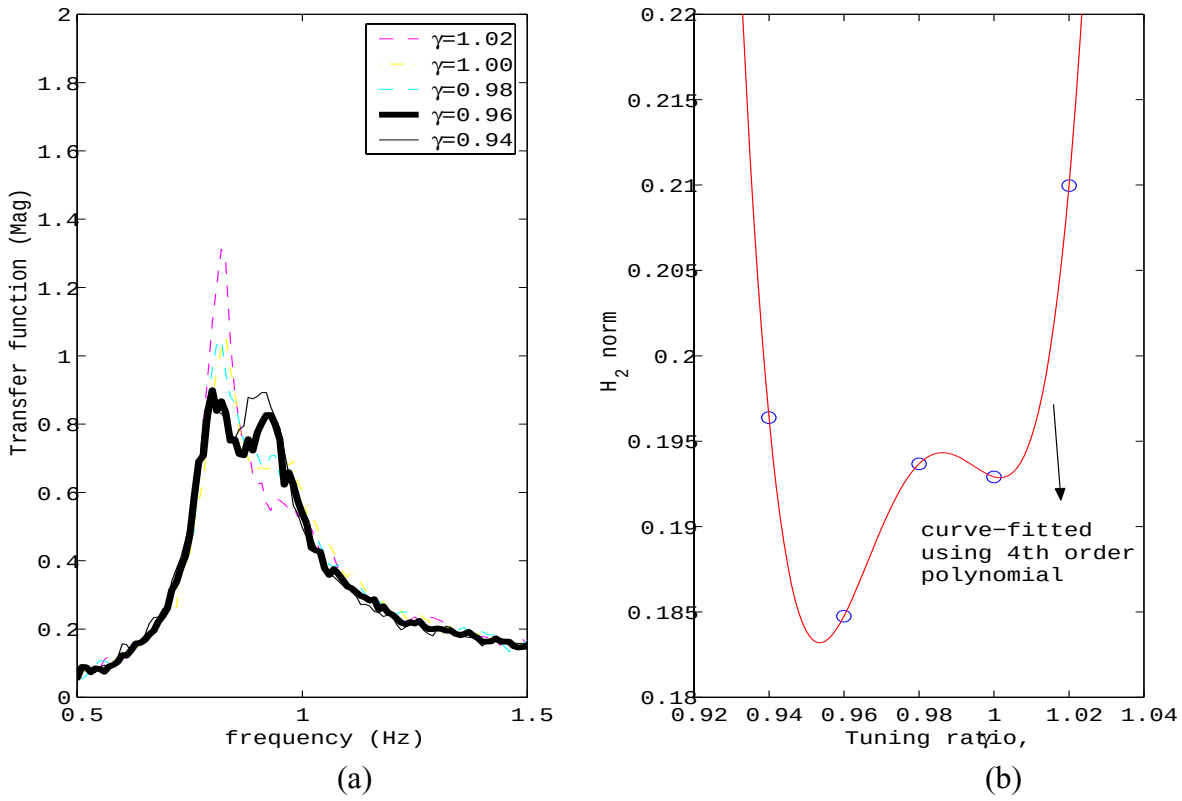

Figure 7.2 (a) Transfer functions for different tuning ratios (b) Variation of H_2 norm with tuning ratio

7.2.2 Effect of damping

The effective damping in the TLCD is obtained through changing the orifice opening of the valve. As noted in previous chapters, the effective damping of the TLCD is an important parameter for optimum absorber performance. The damping is varied by changing the valve angle, where $\theta = 0$ corresponds to fully-open valve and $\theta = 90$ degrees corresponds to fully-closed valve. In the fully-closed position, no liquid oscillations take place and the system becomes a SDOF system. An upper limit of $\theta = 60$ degrees is used in this study. At this position, the valve is almost fully closed. Figure 7.3 shows how the transfer function changes as the valve opening is changed.

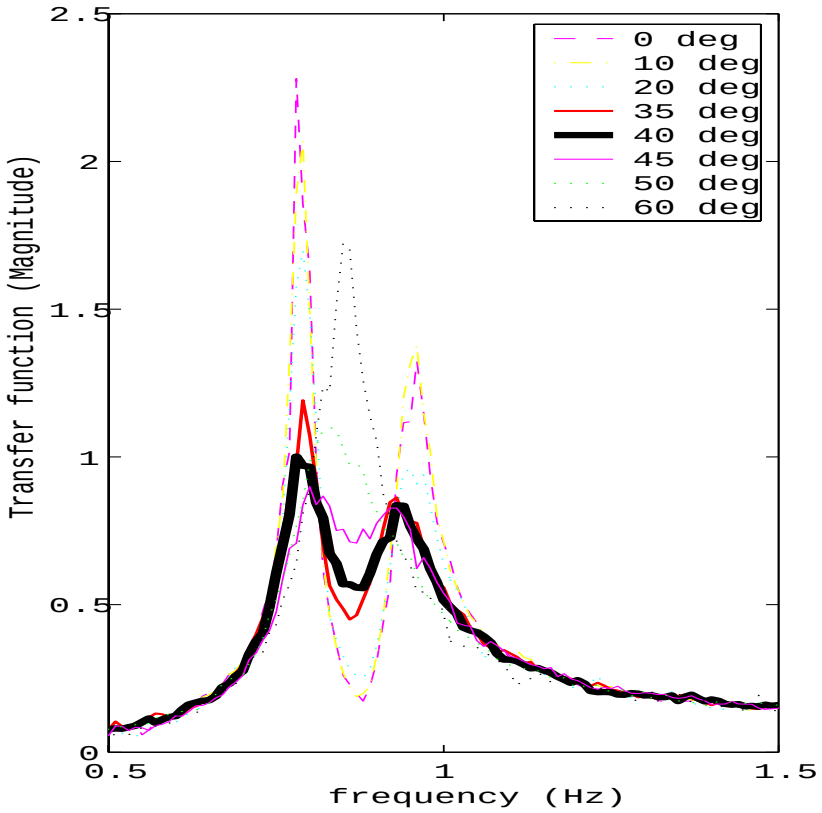

Figure 7.3 Transfer functions for different valve angle openings

7.2.3 Effect of amplitude of excitation

It is well known that the damping introduced by valves and orifices is quadratic in nature. This has been studied experimentally for passive TLCDs (Sakai and Takaeda, 1989; Balendra *et al.* 1995). The damping force is dependent on the liquid velocity,

$$F_d = c|\dot{x}_f|\dot{x}_f \tag{7.2}$$

This implies that the damping introduced by the valve is non-linear and changes as a function of the amplitude of excitation. Figure 7.4 shows the transfer functions of the combined system at two different excitation levels, i.e., S_0 = 0.1 and 0.3 V with different valve opening angles. The transfer functions at θ = 0 degrees (fully-open) are virtually identical

as no nonlinearity is introduced due to the valve. At other valve opening, however, the non-linearity introduced by the valve can be clearly noted.

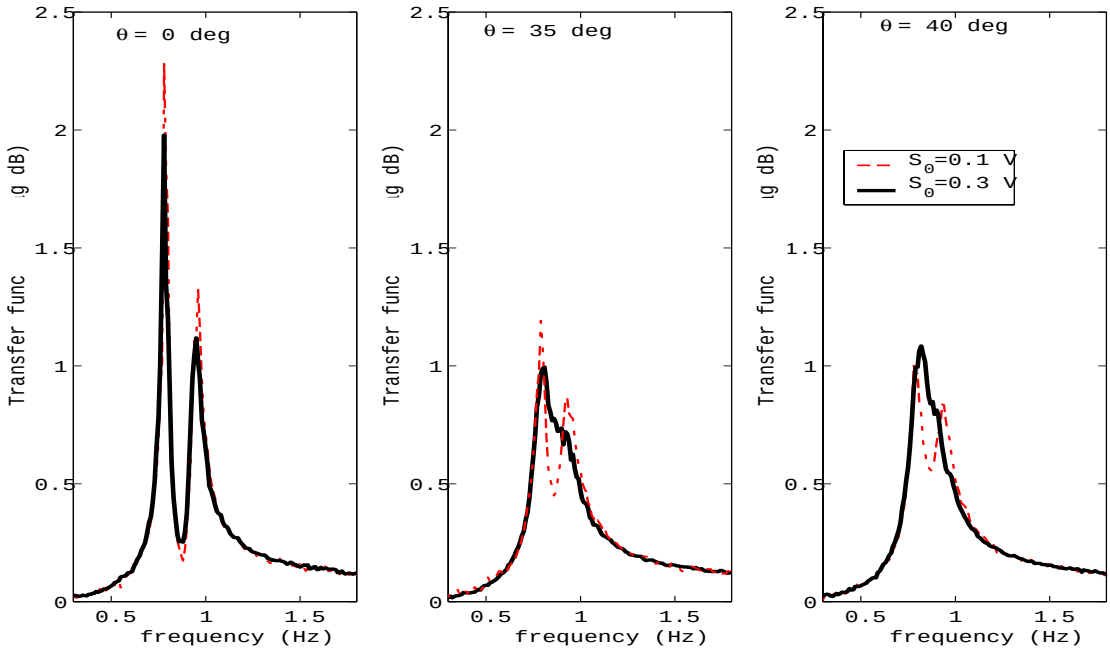

Figure 7.4 Variation of transfer functions for different amplitudes of excitation

From Fig. 7.4, one can note the change in effective damping as the excitation amplitude is varied. Therefore, for the damper to perform optimally at all levels, one needs to determine the optimum damping required at each amplitude of excitation and organized in the form of a *look-up* table. The main idea of a look-up table is to determine the angle of opening which minimizes the $\|H\|_2$ norm of the structural response. This corresponds to the optimal valve opening for a particular amplitude of excitation, as shown in Fig. 7.5(a) for $S_0 = 0.1$ V and $S_0 = 0.3$ V. This procedure is repeated for a wide range of amplitudes of excitation. Using these optimal values, one can construct a nonlinear look-up table as shown in Fig. 7.5(b).

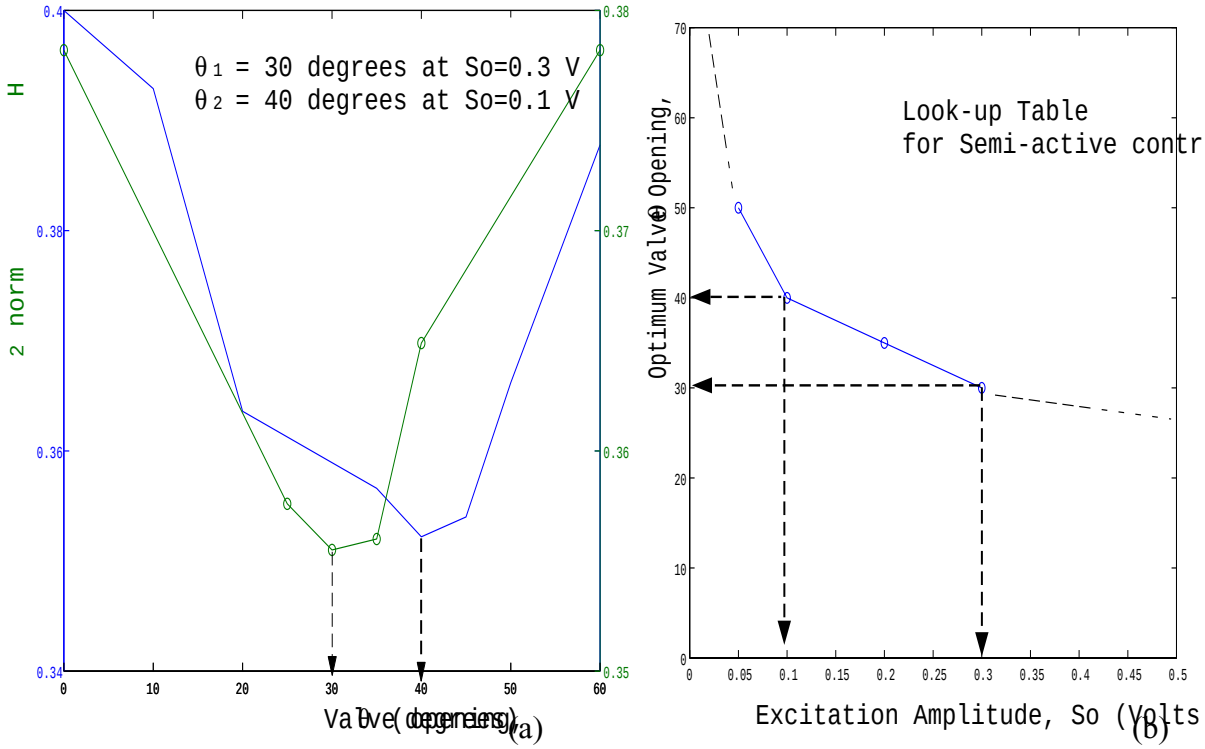

Figure 7.5 (a) Optimization of H_2 norm (b) Look-up table for semi-active control

7.2.4 Equivalent damping

The equivalent damping of the TLCD is a function of the excitation amplitude and the valve opening. An MATLAB^{TM} program was used to curve-fit the experimental transfer function by minimizing the norm of the error function. The equivalent damping was found to range from 2% (for fully open, $\theta = 0$ deg) to 30% (for almost closed, $\theta = 60$ deg). The optimal damping ratio is obtained as 9% ($\theta = 40$ deg at $S_0 = 0.1$ V) as seen in Fig. 7.6(a)). Figure 7.6 (b) shows the transfer function with non-optimal damping (about 30%) which is realized at $\theta = 60$ deg.

Closed-form equations for the case of white noise excitation applied to the primary system were presented in Chapter 3. However, as reported in Warburton (1982), it is known that the optimum absorber parameters that minimize the RMS accelerations of the primary system for a white noise base excitation are the same as those that minimize the

RMS displacements for a white noise excitation applied to the primary system. Therefore, in this study the equations derived in Chapter 3 are used. In the case of an undamped primary system, one can write the expressions for optimal damping and tuning ratio as,

$$\zeta_{opt} = \frac{\alpha}{2}\sqrt{\frac{\mu\left(1+\mu-\alpha^2\frac{\mu}{4}\right)}{(1+\mu)\left(1+\mu-\frac{\alpha^2\mu}{2}\right)}}\ ; \qquad \gamma_{opt} = \frac{\sqrt{1+\mu\left(1-\frac{\alpha^2}{2}\right)}}{1+\mu} \tag{7.3}$$

In the case of $\mu = 0.1$ and $\alpha = 0.56$ and $\zeta_s \approx 0$, optimum values of the absorber parameters obtained from Eq. 7.3 are: $\zeta_{opt} = 8.9\%$ and $\gamma_{opt} = 0.95$, which are close to the experimental values ($\zeta_{opt} = 9.0\%$ and $\gamma_{opt} = 0.953$).

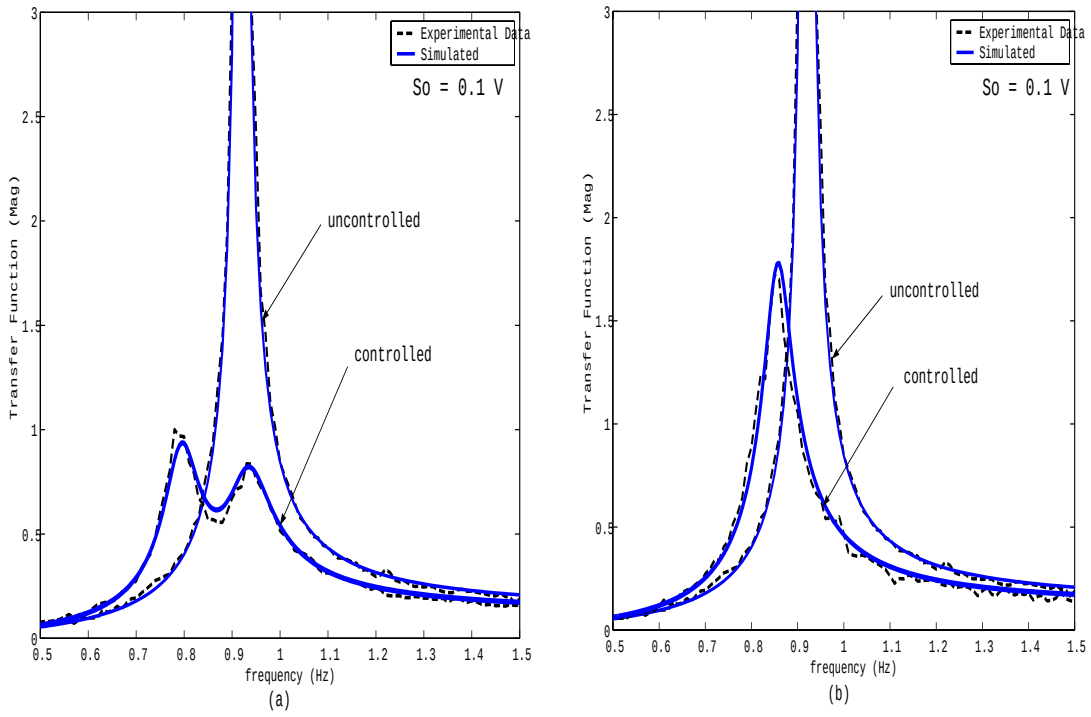

Figure 7.6 (a) Comparison of transfer functions: (a) θ =40 deg, ζ_f = 9 % (optimal damping) (b) θ = 60 deg, ζ_f = 30% (non-optimal damping)

Figure 7.7 (a) shows the 3-D plot of the magnitude of the experimental transfer function as a function of the valve opening angle (and effective damping) and the frequency at $S_0 = 0.1$ Volts. One can observe that the double peaked transfer function changes to a single peak curve as the valve opening angle is increased. Figure 7.7 (b) shows the simulated 3-D transfer function as a function of frequency and equivalent damping ratio. A similar curve is obtained by solving the actual non-linear equations of the TLCD and plotting the dynamic magnification ratio as a function of frequency and the headloss coefficient (for e.g., see Haroun and Pires, 1994). The effect of coalescing of the modal frequencies, from a double peaked curve to a single peaked curve, was also described in chapter 4 while examining the *beat phenomenon* of the combined structure-TLCD system.

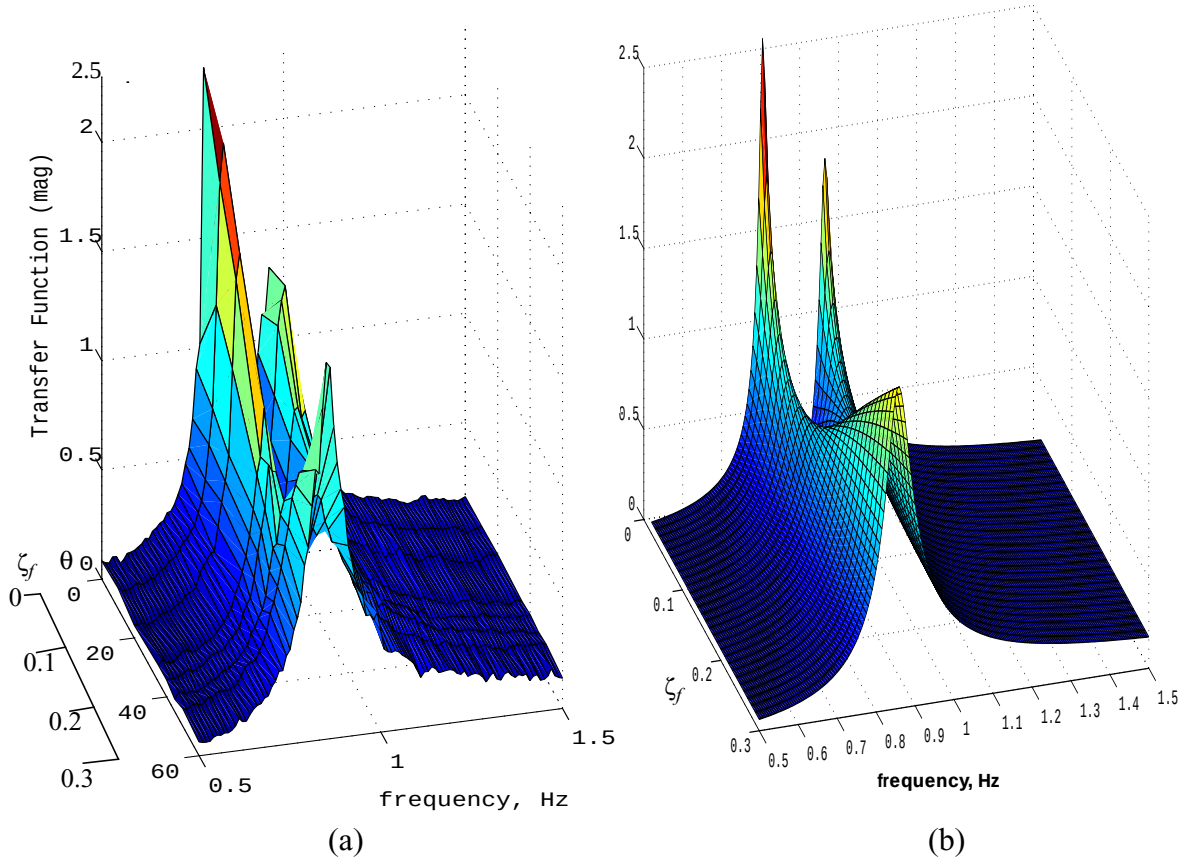

Figure 7.7 3-D plot of transfer function as a function of effective damping and frequency (a) experimental results (b) simulation results.

The experimental results show that the effective damping is a function of the amplitude of excitation and valve angle opening, i.e.,

$$\zeta_f = f(S_0, \theta) \tag{7.4}$$

In section 3.2.1, the expression for the equivalent damping was obtained as:

$$\zeta_f = \frac{\xi \sigma_{\dot{x}_f}}{2\sqrt{\pi g l}} \equiv f(\sigma_{\dot{x}_f}, \xi) \tag{7.5}$$

From the Appendix A.3, one can note that the headloss coefficient is a function of the valve opening angle, i.e.,

$$\xi = f(\theta) \tag{7.6}$$

while the standard deviation of the liquid velocity is related to the amplitude of excitation by Eq. 3.9,

$$\sigma_{\dot{x}_f} = f(S_0) \tag{7.7}$$

Therefore, it follows that,

$$\zeta_f = f(S_0, \theta) \equiv f(\xi, \sigma_{\dot{x}_f}) \tag{7.8}$$

Note that the damping is dependent on $\sigma_{\dot{x}_f}$ which in turn is dependent on ζ_f implying that the relationship in Eq. 7.8 is a nonlinear function.

7.3 Experimental Validation

The next step was the experimental validation of the control strategy outlined in Chapter 5. The main idea was to benchmark the performance of the semi-active system to a purely passive system. In the case of a passive system, the headloss coefficient was kept constant. For the semi-active case, the valve opening was changed according to the look-up table developed in Fig. 7.5 (b).

Two different loading time-histories were chosen. The first time history, referred to as case 1, comprised of segments of 20 sec each in length of 0.1 and 0.3 V RMS excitations, while the second time history (case 2) comprises of segments 40 sec each in length of 0.1 and 0.3 V RMS excitations. The underlying objective was to show that the semi-active TLCD, which changes the headloss coefficient in response to changes in external excitation, performed much better than a passive TLCD.

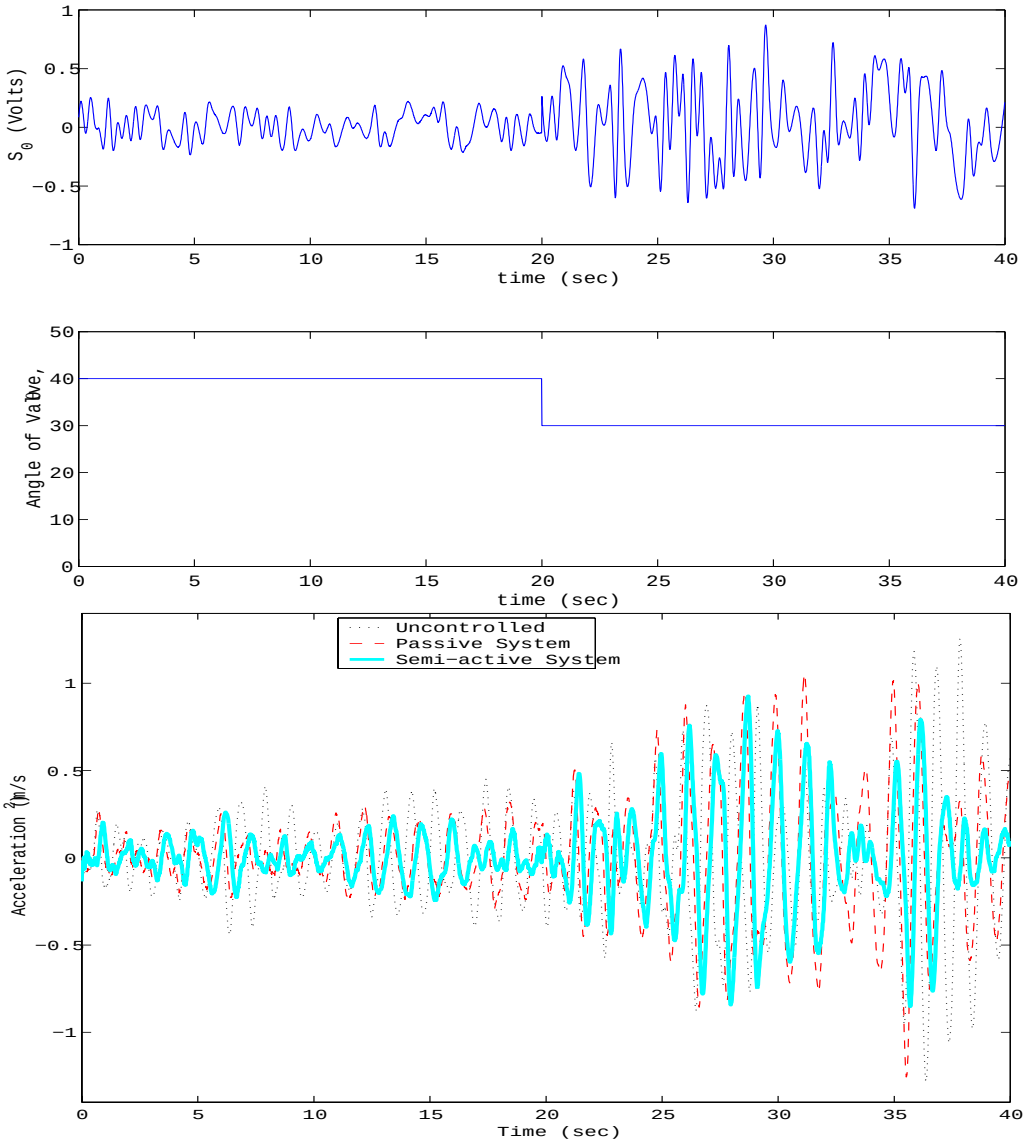

Figure 7.8 Excitation time history, valve angle variations and the resulting accelerations for uncontrolled, passive and semi-active systems for case 1.

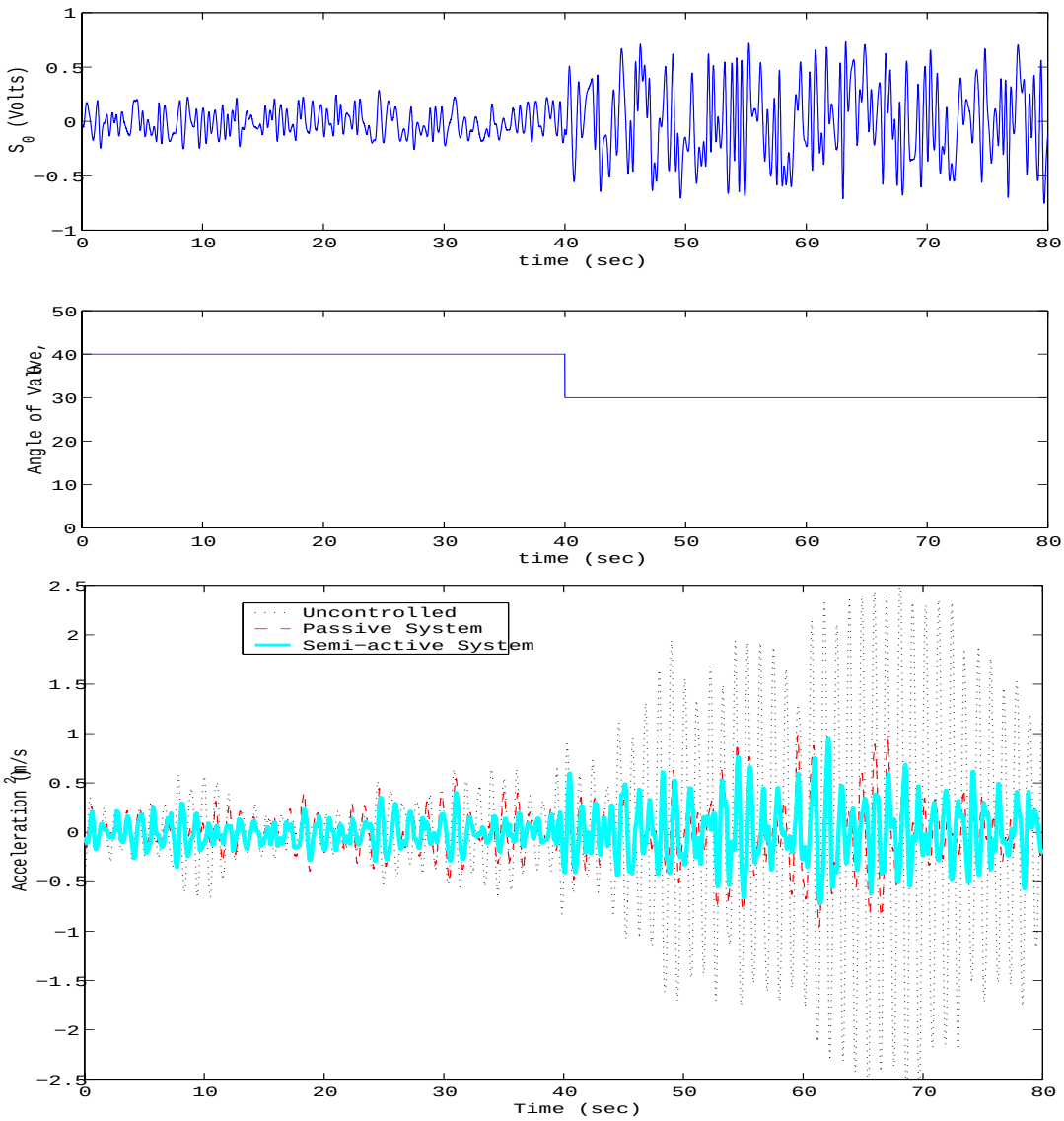

Figure 7.9 Excitation time history, valve angle variations and the resulting accelerations for uncontrolled, passive and semi-active systems for case 2.

From Figs. 7.8, 7.9 and Table 7.1, one can note that for 0.3 V, there is hardly any response reduction for the case 1, while there is a 76% reduction for case 2. This is because case 2 record is of a longer duration and hence the steady-state of the response is established. This increases the liquid damper effectiveness as liquid oscillations are fully developed. One can also see that at higher levels of excitation, the optimum damping is close to the passive system damping, therefore the improvement of semi-active system is

not substantial (about 13% improvement over passive system). On the other hand, for lower levels of excitation, the improvement is more drastic (about 27% improvement over passive system). The overall RMS response reduction of semi-active system over passive system was 23% for case 1 and 15% for case 2.

It is noteworthy that the response reduction of 76% is high. This is because the mass ratio of the damper considered in the scaled-down experiment was 10%. This is a very high mass ratio since in most typical buildings, a mass ratio of approximately 1% can be accommodated due to the weight and space requirements. However, in this study, a comparison of the performance of passive and semi-active systems was performed. Numerical studies indicate, however, that a 1% mass ratio would provide about 45% reduction in response. A similar analytical study was performed in Chapter 5 (Section 5.3.1), where an improvement of 20% was noted for a semi-active system over a passive system using a TLCD mass ratio of 1%.

TABLE 7.1 Performance of semi-active system as compared to uncontrolled and passive system

	RMS (cm/s^2)	**Peak (cm/s^2)**	**RMS (cm/s^2)**	**Peak (cm/s^2)**	**RMS (cm/s^2)**	**Peak (cm/s^2)**
Case 1	**segment 1: First 20 sec**		**segment 2: Next 20 sec**		**Total 40 sec**	
Uncontrolled	20.17	45.08	46.65	125.57	35.94	125.57
Passive	13.69 (32.1%)	32.0 (29%)	45.30 (2.8 %)	105.25 (16.2 %)	33.46 (6.9 %)	105.25 (16.2 %)
Semi-Active	10.09 (50.0 %)	26.34 (41.6 %)	34.95 (25.08 %)	92.76 (26.1 %)	25.73 (28.4 %)	92.76 (26.1 %)
Case 2	**segment 1: First 40 sec**		**segment 2: Next 40 sec**		**Total 80 sec**	
Uncontrolled	27.69	64.49	125.72	262.67	91.03	262.67
Passive	17.04 (38.5 %)	55.34 (14.2 %)	34.73 (72.3 %)	100.12 (61.8 %)	27.35 (69.95 %)	100.12 (61.8 %)
Semi-Active	12.56 (54.6 %)	40.86 (36.64 %)	30.2 (75.97 %)	95.02 (63.8 %)	23.15 (74.56 %)	95.02 (63.8 %)

7.4 Concluding Remarks

An experimental investigation to determine the optimal absorber parameters of the combined structure-TLCD system was presented. The experimental results were compared to the previously obtained analytical results. A control strategy based on a gain-scheduled look-up table was verified experimentally. It was observed that at low amplitudes of excitation, the TLCD damping was enhanced by constricting the orifice and at higher amplitudes by dilating the orifice to supply the optimal damping. Experimental studies have shown that the semi-active TLCD can boost the performance of the passive TLCD by an additional 15-25% and maintains the optimal damping at all levels of excitation. This justifies the additional costs of using sensors and controllable valves in the semi-active system. A more detailed cost and implementation comparison is discussed in Chapter 8.